Norsk Geografisk Tidsskrift–Norwegian Journal of Geography Vol. 58, 61–73. Oslo. ISSN 0029-1951

GIS-based modeling of glacial hazards and their interactions using Landsat-TM and IKONOS imagery

CHRISTIAN HUGGEL, ANDREAS KÄÄB & NADINE SALZMANN

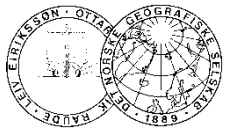

Huggel, C., Kääb, A. & Salzmann, N. 2004. GIS-based modeling of glacial hazards and their interactions using Landsat-TM and IKONOS imagery. *Norsk Geografisk Tidsskrift–Norwegian Journal of Geography* Vol. 58, 61–73. Oslo. ISSN 0029-1951.

Hazard interactions in glacial and periglacial environments are of crucial importance due to their potential for causing major catastrophes. Nevertheless, glacial and periglacial hazards have usually been modeled separately to date. In this study, we therefore propose a methodological strategy for modeling and assessing glacial and periglacial hazard interactions on a regional scale, including ice avalanches, lake outbursts and periglacial debris flows. Due to climate-related rapid changes in glacial and periglacial areas, methods which incorporate monitoring capacities are needed. Hence, the methods presented here are based on remote sensing data, which are particularly powerful for monitoring tasks, and GIS modeling. For ice avalanche and lake-outburst hazard detection and modeling, we applied recently published methods based on Landsat-TM imagery, terrain modeling and flow routing. For detection of potential debris-flow initiation zones in steep debris reservoirs, we present a novel method based on image processing of IKONOS data and terrain modeling, followed by flow modeling. Using this method, we achieve the synthesis of the individual process modeling in order to assess the potential interactions. The modeling is applied to a study region in the central Swiss Alps. The results show that systematic modeling based on remote sensing and GIS is suitable for first-order assessment of glacial and periglacial hazard interactions as well as assessments of possible consequences, including impacts on traffic routes and other infrastructure. Based on this, critical cases can be detected and analyzed by subsequent detailed studies.

Keywords: *GIS modeling, glacial hazards, process interactions, remote sensing*

Christian Huggel, Andreas Kääb, Nadine Salzmann, Glaciology and Geomorphodynamics Group, Department of Geography, University of Zurich, Winterthurerstr. 190, CH-8057 Zürich, Switzerland. E-mail: chuggel@geo.unizh.ch

Introduction

High mountains are characterized by a large mass turnover and thus represent highly dynamic systems (Haeberli 1996). The processes which drive the mass turnover potentially represent serious hazards when interacting with human systems (Greminger 2003, Petraschek & Kienholz 2003). We focus here on the glacial and periglacial areas of high mountains. Glacial and periglacial environments react sensitively to climate change due to the propensity for melting of surface and subsurface ice. Climate change can increase the mass turnover of such areas, change the hazard potential, and shift hazard initiation and adversely affected inhabited zones (Haeberli & Burn 2002, Kääb et al. in press). For hazard assessments, it is of particular importance to assess the possible interactions of different hazardous processes. Some of the most devastating high-mountain catastrophes have, in fact, resulted from such process combinations and chain reactions, as various case studies have documented (Lliboutry et al. 1977, Röthlisberger 1981, Clague & Evans 2000, Richardson & Reynolds 2000a, Kääb et al. 2003a). However, hazard assessments do often not adequately take into account potential process interactions. Hence, there is a need for a methodological framework which incorporates a robust modeling environment and updated information basis representing the current state of high-mountain systems.

We believe that the combination of Geographic Information Systems (GIS) and remote sensing is an effective tool to address this need because of the integration of different spatial and temporal information, up- and downscaling capabilities, and because of the monitoring possibilities. To date, hazards from high-mountain mass transport processes usually have been individually identified and modeled. Here we are referring to the following processes: ice avalanches, glacial lake outbursts and periglacial debris flows from large debris reservoirs. Problems related to the assessment of ice avalanches and glacial lake outbursts have recently been discussed and corresponding methods presented (Margreth & Funk 1999, Huggel et al. 2003a, Salzmann et al. 2004, this issue). For ice avalanches and glacial lake outbursts, we follow the approaches by Salzmann et al. (2004) and Huggel et al. (2003a), respectively. However, recent modeling approaches for regional-scale debris flow initiation, based on topographic/topologic parameters (Heinimann et al. 1998, Oswald 2001) and statistical multivariate models (Bathurst et al. 2003), often cannot be applied to periglacial zones since debris flow initiation in large periglacial debris reservoirs and at the contact zone with bedrock has different characteristics, as we show below. Therefore, a major focus of this paper is the identification and modeling of debris flow initiation areas in periglacial environments. For this purpose, we present a method for automatic identification of steep debris reservoirs potentially prone to debris flow initiation, based on very-high resolution satellite data and followed by modeling of corresponding potential debris flows. Subsequently, we attempt a synthesis of the individual approaches: having detected the hazard source areas and having simulated the different processes, we try to model the interactions of these processes. As a result, the critical chain reaction processes are identified and the potential impact can be estimated. Interactions involving rockfall, snow avalanches, or landslides are beyond the scope of this study. The scale of the study is regional. Thus, we indicate where critical situations may emerge and assess possible consequences. It is not

Taylor & Francis
Taylor & Francis Group

DOI 10.1080/00291950410002296

the goal to perform a detailed hazard assessment of a certain site. Instead, our objective is to present a combination of techniques and to describe the application on selected examples. Information on infrastructure (e.g. roads) is included in the modeling.

We first present the data used and the different modeling approaches for the individual processes, and subsequently for the process interactions. The models are then applied to the Grimsel-Susten region in the Bernese Alps, Switzerland. Finally, the results are discussed.

Study region and data

The study region is located in the central Swiss Alps in the area of the Grimsel Pass (Fig. 1). The upper Hasli valley, through which the Grimsel Pass highway runs and where the River Aare has its origin, dominates the study region. Selected sites investigated here are located in tributaries to the main Hasli valley. The western part of the study region includes the Urbach valley ending up at Gauli glacier. The region is characterized and hydrologically connected by a hydropower system operated by Kraftwerke Oberhasli (KWO). KWO has been in operation since the 1930s and is one of the major hydropower companies in Switzerland. In addition to (natural) glacial and periglacial lakes, a series of reservoir dam lakes are situated in the region (Fig. 1).

With regard to remote sensing data, a 1998 Landsat Thematic-Mapper scene of 28.5 m spatial resolution was used (track 195/frame 28; August 31 1998). Landsat-TM provides seven spectral channels, three of which are located in the visible range and four in the near, middle and thermal infrared. Close-up studies were performed with IKONOS imagery. Together with QuickBird, IKONOS is currently the only commercially available satellite sensor with spatial resolution in the range of 1 m (Dial et al. 2003). In this study we used an IKONOS panchromatic image (1 m resolution, visible range) recorded on 17 September 2000.

As digital terrain data, the 25-m gridded DEM25, Level 2, distributed by the Swiss Federal Office of Topography (Swisstopo), was used. It entirely covers the area of Switzerland and is therefore suited for regional applications within Switzerland. In the region of interest, the digital elevation model (DEM) accuracy of DEM25 is given with a vertical RMSE (Root Mean Square Error) between 4 and 6 m (Swisstopo, 2003). Slope values derived from the DEM25 are generally accurate to within 1° to 2°.

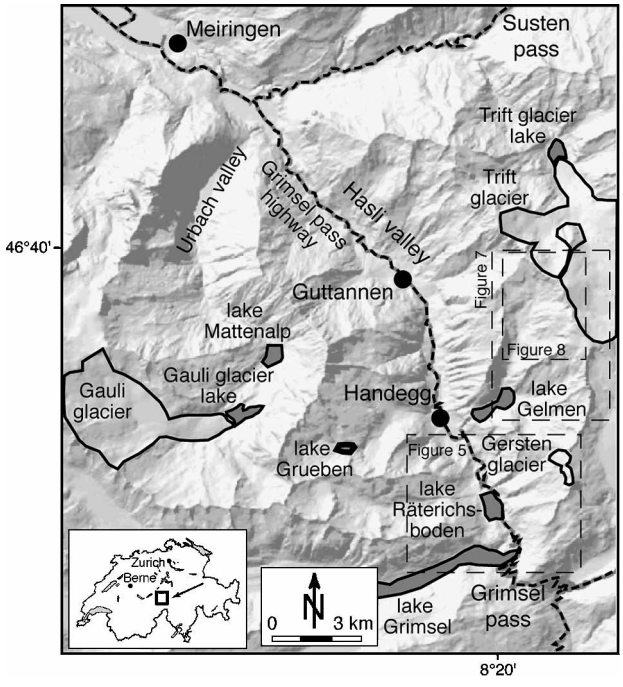

Fig. 1. Overview map of the study region depicting lakes and glaciers referred to in this study, and the main traffic routes.

Models

Ice avalanches

In this study, ice-avalanche modeling consists of detection of steep glaciers on the basis of multispectral remote sensing data and digital terrain modeling, and simulation of the avalanche process starting at the glaciers detected along a modeled trajectory.

The avalanche starting conditions depend on the type of failure. According to Alean (1985) and Haefeli (1966), ice break-off may result from two main morphological types of potential ice avalanche starting zones: ramp-type and cliff-type glaciers. Cliff-type glaciers are characterized by a marked break in slope of bedrock and/or ice. The glacier develops a nearly vertical front. Ice break-off processes relate to high normal stresses at the front with crevasse formation rather than to the slope of the glacier bed or surface. Such glacier fronts experience frequent small-size processes of ice breaking off (Deline et al. 2002).

Ramp-type glaciers are situated on a more-or-less uniformly inclined plain. The failure mechanism is due to sliding or shearing of an ice mass on or near the bedrock after reduction in shear strength (Haeberli et al. 1999, Margreth & Funk 1999). The occurrence of ramp-type ice avalanches suggests a dependency on the inclination of the glacier bed and on temperature conditions within and at the base of the glacier (Alean 1985). Accordingly, the critical bed slope of avalanching glaciers has been observed to increase with increasing altitude (Alean 1985). Temperate glaciers have been found to produce ice avalanches from a minimum slope of *c.*25°, and cold-based glaciers from *c.*45° (Alean 1985). Climatic change, i.e. atmospheric warming and/or intense liquid precipitation, may imply higher amounts of water at the base of the glacier, and thus unfavorable stress changes and possibly failure (Haeberli et al. 1999). The critical bed slope indicated here will therefore need re-assessment in the future.

Detection of glaciers is achieved using Landsat-TM imagery. Previous studies have shown that an algorithm applying the ratio of TM bands 4 and 5 provides robust results for mapping of glacierized areas (Hall et al. 1988, Jacobs et al. 1997, Paul et al. 2002). Automated glacier

mapping is enabled by segmentation (thresholding) of the TM4/TM5 ratio image (Paul et al. 2002). Here, a threshold of 2.2 was used to segment glacierized areas. The following post-processing algorithms were then applied to improve the results: (i) elimination of misclassified pixels (e.g. in shadowed vegetated areas), by segmentation of the hue component of a IHS-transformation of TM bands 5,4,3; (ii) elimination of misclassified pixels in lakes by using a lake mask (see the following section); (iii) application of a 3×3 median filter for elimination of isolated glacier pixels (Paul et al. 2002).

For identification of potentially avalanche-prone glaciers, the DEM25 was combined with the glacier map to select those glacier areas with slopes greater than 25°. These potentially hazardous glaciers subsequently feed the model as avalanche starting zones.

Ice avalanche trajectory and runout modeling is fully implemented in a GIS Arc/Info environment. The trajectory is modeled according to a routing algorithm which assigns flow from each cell to one of its eight neighbors, either adjacent or diagonal, in the direction of the steepest descent. This method, designated D8 (eight possible flow directions), was introduced by O'Callaghan & Mark (1984) and is still one of the most frequently used (Marks et al. 1984, Jenson & Domingue 1988, Tarboton et al. 1991). For determination of the avalanche runout distance, a simple 1-parameter model is used. Alean (1985) has found that in the Alps the average slope of ice avalanche trajectories does not fall below 17° ($\tan\alpha = 0.31$). Thereby, the average slope describes the angle with the horizontal of a line from the top of the starting zone to the furthest point of deposition. Outside the Alps, this minimum value may be under-run in extreme cases (Körner 1983). In particular, the recent ice avalanche in the Kazbek massif in the Russian Caucasus showed that an average slope as low as 8.5° ($\tan\alpha = 0.15$) is possible under especially adverse conditions (Kääb et al. 2003a). For application within the Alps we model the probable maximum runout distance based on an average slope of 17°.

Glacial lake outbursts

Similarly to ice avalanches, glacial lake outbursts are modeled by first detecting and mapping the potentially hazardous lakes, followed by a simulation of the outburst flood. For detection of potentially hazardous lakes, an approach by Huggel et al. (2002) was followed. Thereby, a Normalized Difference Water Index (NDWI), which uses the spectral TM bands 1 and 4, was applied. Misclassifications resulting from pixels in shadow can be eliminated by computing a cast-shadow mask using a 25 m DEM to simulate the sun position at the time of satellite overpass. The lake volume is estimated based on a statistical relationship between lake volume and area (Huggel et al. 2002). A set of decision criteria was then applied to evaluate the hazard potential of the lakes and to decide whether an outburst flood is modeled. For instance, lake size, lake and dam geometry, or dam type are important parameters to consider (Richardson & Reynolds 2000a, Huggel et al. 2002).

The basic idea is then to propagate flow from the source location downstream until a certain empirically defined point of runout is reached. The modified single flow (MSF) model applied here was developed by Huggel et al. (2003a). The algorithm is based on a single flow direction approach (O'Callaghan & Mark 1984, Jenson & Domingue 1988), where the central flow line follows the direction of steepest descent. However, debris flows show spreading flow behavior in less steep terrain which cannot adequately be simulated by a single flow direction algorithm. Therefore, a function was integrated that enabled flow diversion of up to 45° from the steepest descent direction (Huggel et al. 2003a). A linear function defines that the more the flow diverts from the steepest descent direction the greater is the resistance. Flow resistance is then related to a probability function which basically defines that the more flow resistance that has to be overcome to reach a point the less likely is it affected by the flow (Huggel et al. 2003a). The model is thus capable of simulating the different characteristics of debris flows in confined channel sections (largely limited spread due to converging flow) and on relatively flat or convex terrain (e.g. debris fans; greater spread due to more diverging flow), and to provide corresponding probabilities.

The modeled debris flow is stopped when an average slope of 11° ($\tan\alpha = 0.19$) is reached. This value is based on studies that analyzed the runout characteristics of debris flows from glacier/moraine-dammed lakes in the European Alps and found a minimum slope of 11° (Haeberli 1983, Huggel et al. 2002). The average slope is applied irrespective of the streamflow connectivity in the modeled trajectory. However, if the debris flow reaches a receiving stream in the main valley, the slope criterion of 11° might no longer apply, and has to be re-assessed. Floods with weight of sediment $<$weight of water commonly show a more attenuating runout behavior and are not modeled here due to the high sediment availability in the flow trajectories of the study region.

Periglacial debris flows

Modeling of periglacial debris flows implies detection of steep reservoirs of loose sediment (e.g. moraines, scree slopes) and subsequent simulation of flow trajectory and runout. Periglacial zones with large accumulation of loose and unconsolidated material are particularly prone to debris flow formation, and often show larger flow events that may reach inhabited areas at the bottom of the main valley (Haeberli et al. 1991, Zimmermann et al. 1997). Since the Little Ice Age maximum in *c*.1850, glaciers have retreated substantially and exposed large areas of morainic, unconsolidated sediment (Evans & Clague 1994). Investigations of the severe and repeated debris flow disasters in the Swiss Alps in 1987 have shown that more than 50% of debris flows greater than 1000 m^3 originated in zones still covered by glaciers 150 years ago (Haeberli et al. 1991, Zimmermann & Haeberli 1992). Poorly sorted debris accumulations are usually characterized by a heterogeneous, rather permeable, loose and porous structure (Oberholzer et al. 2003). The hydrological conditions in cohesionless material are important for debris flow formation, the material being influenced by inhomogenities and changing permeability within the

meter and decimeter range (Rickenmann & Zimmermann 1993). In cases of enhanced water input, locally saturated zones can form and lead to instabilities. In fact, Haeberli et al. (1991) have found that debris flow initiation in periglacial zones has been mainly related to large, very poorly consolidated debris accumulations which were furthermore unfrozen, hydraulically inhomogeneous and permeable. The debris flow size, however, seems to be limited by the flow dynamics rather than by the internal structure of the scree slope.

In addition, permafrost and melting of permafrost under conditions of atmospheric warming can affect debris flow activity. Zimmermann & Haeberli (1992) found that the 1987 debris flows predominantly formed at locations where permafrost is absent or marginal. Active layer instability processes have been observed only at two sites. Permafrost thawing and related depth increase of the active layer, as well as incomplete thaw consolidation after melt, may increase both frequency and magnitude (higher potential erosion depth) of debris flows (Zimmermann et al. 1997). However, permafrost also acts as a barrier to groundwater percolation and can imply local saturation within the non-frozen debris. Permafrost degradation can thus reduce debris flow initiation.

A determinant factor for debris flow initiation is the slope gradient of a debris accumulation. Rickenmann & Zimmermann (1993) investigated the starting conditions of debris flows and found that debris flows originating in large and steep debris reservoirs such as talus or scree slopes have typical starting slope inclinations of between 27° and 38°. For debris flows initiating at the contact zone between a rock wall and a talus slope, starting slopes lie in a similar range. Generally, these slope values have been confirmed by other investigations (Takahashi 1981, Hungr et al. 1984) and are also related to the angle of repose associated with the grain size of the material involved. To summarize, the starting conditions of debris flows with origins in periglacial areas can significantly differ from lower-land debris flows. Topographic criteria for debris flow initiation in lower-elevation zones, such as relative distance from a flow channel or terrain concavity (curvature) (Heinimann et al. 1998, Bachmann 2001), may not apply to debris flow initiation types in periglacial zones, and therefore different approaches had to be found here.

The detection of steep sediment reservoirs from remote sensing imagery is a major challenge. A main problem is the spectral similarity of bare rock and debris (Paul et al. 2004). Therefore, classification algorithms considering spectral information only are unlikely to yield satisfactory results. Recent research efforts directed towards mapping of debris-covered glaciers by remote sensing were confronted with similar problems, and stressed the importance of including digital elevation information for classification (Bishop et al. 1999, Paul et al. 2004). In this study, we first evaluated a combined method of artificial neural network (ANN) classification and digital elevation modeling for identification of steep periglacial debris reservoirs. We used a feed-forward back-propagation network with two hidden layers (each with 15 nodes) (Pao 1989). The success of the ANN classification was generally limited. Tests with textural analysis of Landsat-TM for supporting automated classification have largely failed as well and even visual image interpretation can be very difficult.

For multispectral data with a spatial resolution of 20 to 30 m, an improved discrimination between debris and rock is enabled by the definition of a threshold slope between rock and debris zones. In high-mountain areas, debris predominantly originates from the weathering processes of surrounding rock walls and subsequent transport processes. Related rockfalls typically build up debris cones, whose slopes are limited by the stability of loose debris (*c*.30°). Rockwalls, on the other hand, have been found to be best represented by a minimum threshold slope of 34° (Heinimann et al. 1998, Zemp 2002). The upper slope range for debris flow initiation in talus slopes was previously defined as 38°. We therefore tested both 34° and 38° as a debris-rock threshold slope by intersecting the slope ranges with the ANN classification of debris and rock. Since the potential for debris flows is modeled here, availability of water – important in influencing runout – is assumed to be given for a particular event. Zimmermann et al. (1997) presented an approach which considered only debris slope areas with catchment sizes $>5000\ m^2$ as debris-flow initiation zones.

The limited success of the ANN classification for detection of steep debris reservoirs stimulated further investigations. The spectral similarity of debris and rock caused the focus to shift to the importance of spatial resolution for detection of debris accumulations. As a function of spatial resolution, debris accumulations show a uniform surface structure in contrast to exposed bedrock. Such uniform structures are not recognised by satellite sensors with spatial resolution of 20 to 30 m, and thus, spatial resolution is a limiting factor for debris reservoir applications when using Landsat-TM. In order to vastly improve the spatial resolution, IKONOS panchromatic data of 1 m resolution was used.

An edge detection filter was found to be able to detect the structural uniformity of debris accumulations, and to discriminate them from the irregular structure of bedrock. The filter calculates the average of the grey value difference between the central pixel and each of its surrounding neighbors, and assigns the value to the central pixel. More uniform areas have smaller grey value differences and are thus assigned lower values. The number of neighbors is defined by a moving window of specified dimensions. Appropriate window size basically depends on the scale of the structure to be detected. In the present study, the best results were obtained by using a 11×11 window. The resulting grey value image was then segmented into debris and bedrock according to a threshold value of 47. Finally, a 5×5 median filter was applied to smooth the classification and avoid small isolated pixels.

For detection of potential debris flow initiation zones, areas with a slope range between 27° and 38° were selected from the previously classified debris accumulation areas. These locations represented the input or source to the modified single flow direction model (cf. glacial lake outbursts) to simulate the impact of a potential debris flow. For the probable maximum runout distance, an average slope of 11° ($\tan\alpha = 0.19$) was used. Several studies have shown that this slope value encompasses debris flow events in the

Swiss Alps (Haeberli et al. 1991, Rickenmann & Zimmermann 1993, Zimmermann et al. 1997). Other approaches relating the critical average runout slope to the catchment area of each cell (Heinimann et al. 1998) are less suitable for our purpose since large periglacial debris reservoirs may have enormous sediment yields that are not directly related to catchment size.

Process interactions

Interaction between the above processes may strongly increase the risk of hazards. The most significant chain reaction in this context is probably the danger from ice avalanches, debris flows, rockfall or landslides reaching a lake and thus provoking a lake outburst. In fact, mass movements may act as outburst trigger mechanisms by producing impact waves and overtopping of the dam (Reynolds 1992, Clague & Evans 2000, Richardson & Reynolds 2000a). We concentrate on ice avalanches and debris flows as lake-outburst triggers. The effects of process interactions have to be analyzed for each case individually. In general, glacial lakes are often particularly susceptible to impact waves due to their steep shores and narrow lake geometries (Fritz 2002). The processes responsible for producing impact waves, run-up on the dam and overtopping are complex and not completely understood (Vischer & Hager 1998). Formation and dimension of impact waves depend on the depth and volume of the lake, on the volume, flow height and velocity of the incoming mass movement, and on the angle of the flow path at which the mass enters the lake. Watts & Walder (2003) and Walder et al. (2003) emphasized the significance of the rate of volume entering the lake and Froude number effects (i.e. supercritical flow). The run-up height on the dam further depends on wave length and height, freeboard height and slope of the dam (Müller 1995). The overtopping volume is related to the run-up height. For estimates of the overtopping volume, it is important to consider the ratio, H, between the volume of the incoming mass and the lake volume. Based on an analysis of case histories (Huber 1980, Müller 1995, Walder et al. 2003), we defined the following ranges for H: For H = 1:1 to 1:10, the lake may be emptied completely. For H = 1:10 to 1:100, there is still a high probability of overtopping when the freeboard is small in comparison to the dam height. As a first approximation, the overtopping volume may be considered equal to the incoming mass.

It is beyond the scope of this study to provide a detailed analysis of flow dynamics of the mass movements and related effects in the lake. Instead, it is intended to indicate where critical situations may emerge, and if possible, to model related processes. Rough estimates of flow volume of the incoming mass and lake volume can be supported by high to very-high resolution remote sensing data and empirical relations (e.g. IKONOS, aerial photography) (Huggel et al. 2002), and flow velocities can be approximated by basically distinguishing between avalanche and debris flow processes. Avalanches usually reach velocities between 15 and 100 m/s, whereas debris flows commonly move at speeds of *c*.3 to 15 m/s. The slope of the flow path is available from digital elevation models (DEMs).

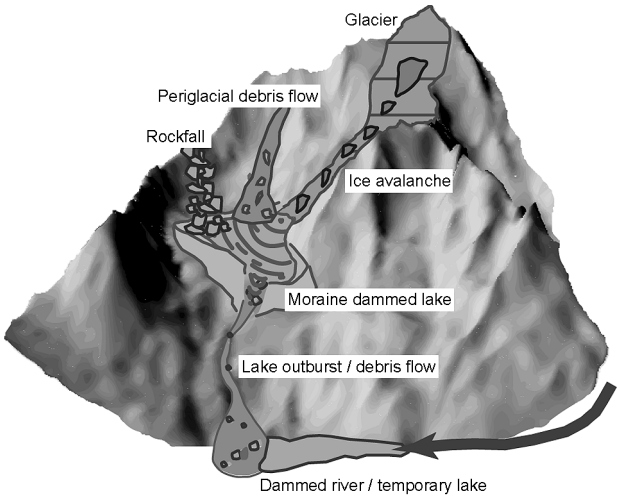

Fig. 2. Schematic overview showing potential interactions of hazardous processes in a glacial and periglacial environment.

Other important process interactions relate to ice avalanches, or possibly debris flows, blocking river channels. Temporary lakes can form behind such dams and cause sudden, very high discharges in cases of rupture. Further hazardous process interactions not specifically considered here are, for instance, snow avalanches and rockfall into a lake, rockfall onto a glacier, flow transformation of ice avalanches into snow and debris avalanches/flows, or debris flows into hyperconcentrated flows, or vice versa (Körner 1983, Pierson & Scott 1985, Haeberli et al. 1997, Kääb et al. 2003a). Fig. 2 provides a schematic overview of potential interactions in a glacial and periglacial environment. Fig. 3 shows the work flow of the different methods to assess hazards from ice avalanches, glacial lake outbursts, periglacial debris flows, and the resulting process interactions.

Model applications

Ice avalanches

The ice avalanche model was applied to the whole study region but for better comprehension, a specific case at Räterichsboden, in the Grimsel region, was selected. In 1962, the reservoir lake Räterichsboden was hit by a major snow avalanche (*c*.300,000 m^3) which penetrated the ice on the lake surface and caused run-up waves and possibly dam overtopping (Müller 1995). Presently, two small glaciers in a west-exposed cirque under Gerstenhörner mountain (3189 m a.s.l.) show potentially avalanche-prone areas with slopes between 25° and 34°.

A more detailed analysis based on the IKONOS image indicates that the glaciers can be considered relatively stable. Though a few crevasses can be identified on the image, no indication of instability was found (Fig. 4). However, assessment of the stability of steep glaciers is highly complex and difficult. The 1989 ice avalanche at Glacier de Coolidge showed that a small cirque glacier with relatively moderate

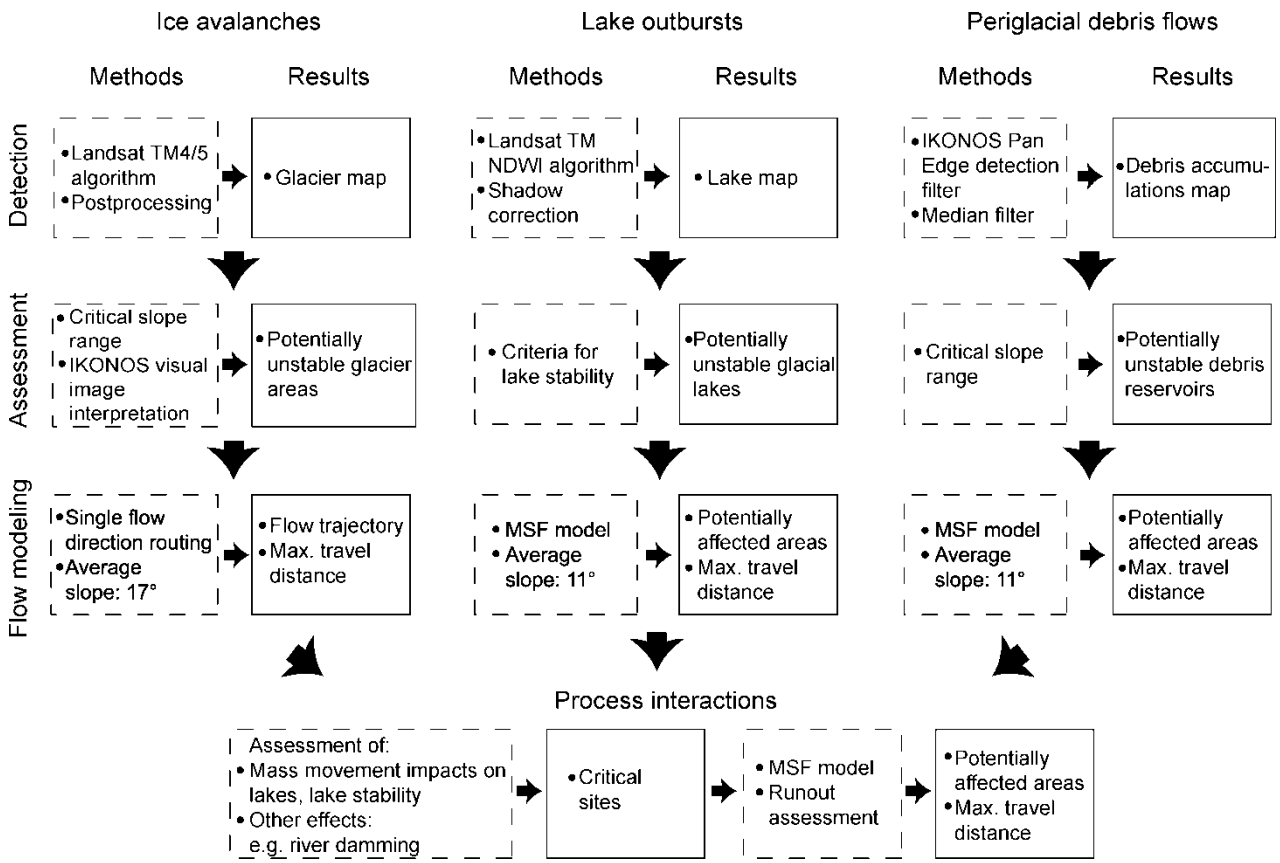

Fig. 3. Work flow integrating the methods for assessment of hazards from ice avalanches, glacial lake outbursts, periglacial debris flows and resulting process interactions.

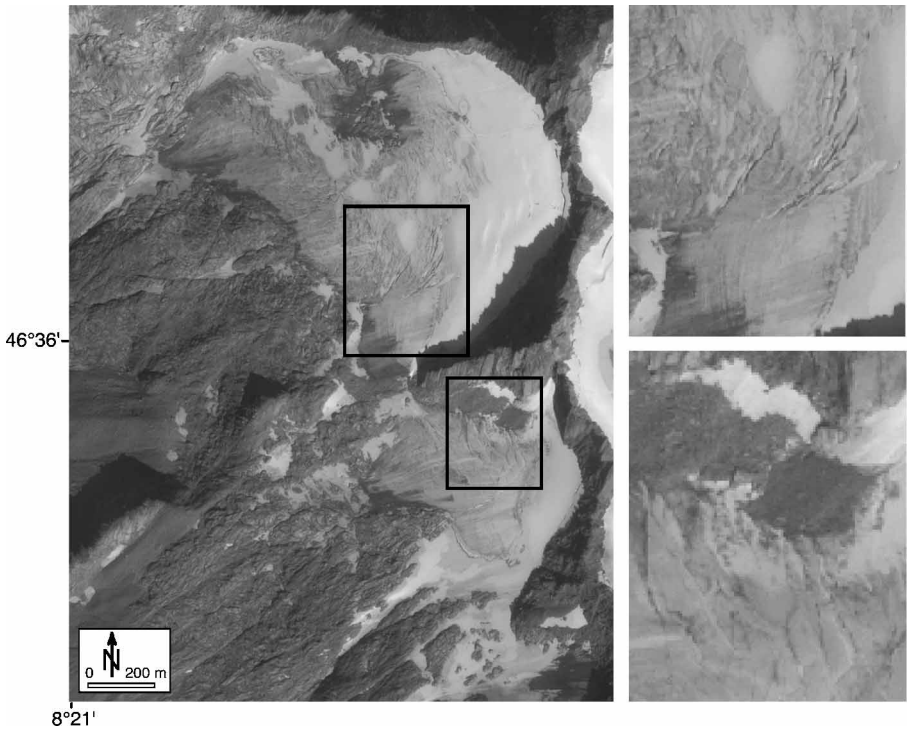

Fig. 4. IKONOS image (panchromatic channel) from Gersten glacier from 17 September 2000. Crevasses zones recognizable on the image are shown enlarged on the right-hand side.

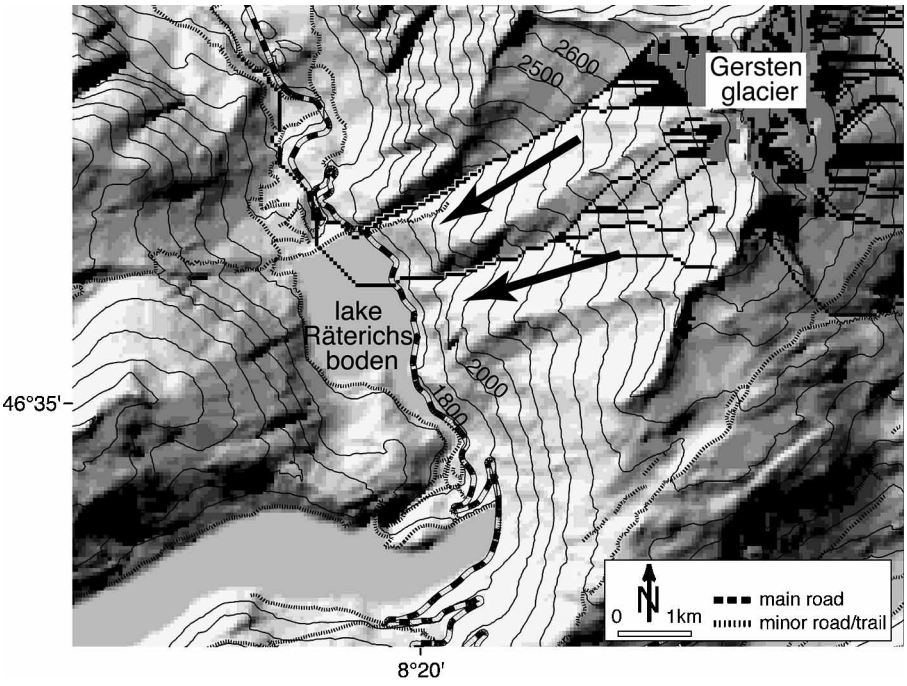

Fig. 5. Modeled ice avalanche from Gersten glacier reaching lake Räterichsboden. The empirically-based determination of the avalanche travel distance predicts a runout beyond lake Räterichsboden without considering the dam structures. Potentially unstable glacier ice is shown in light grey, ice avalanches in black. Arrows indicate the direction of the flow trajectory of ice avalanches.

inclination (*c*.23°) can fail as a whole (Dutto et al. 1991). Subglacial hydrological conditions are likely to be a determinant factor (Haeberli et al. 1999, Funk & Minor 2001). In our case, the potential ice avalanche volume would thus involve the whole glacier in an extreme case. Based on an estimated average depth of 10 to 20 m, the ice volume amounts to 2 to 4 million m^3 for the northern glacier and 0.7 to 1.4 million m^3 for the southern glacier.

The modeled avalanche trajectory leads directly into the reservoir lake Räterichsboden (Fig. 5). The following considerations have to be taken into account in relation with the potential hazard. The average slope of the trajectory from the Gersten glacier to Räterichsboden is rather steep (22° to 25°), and a potential ice avalanche has thus higher probability to actually reach the lake. The Grimsel Pass road above the lake could also be affected by an ice avalanche. While snow avalanches are limited to winter or spring, ice avalanches have equal, and in this case likely higher, probability of occurring in summer than in winter, and may flow along different tracks than the better-known snow avalanches usually flow along. Furthermore, reservoir lakes are usually more vulnerable during summer because lake levels are higher than in winter due to higher water input and lake level lowering in winter for safety reasons related to snow avalanche impacts. A hazard aspect which should be taken into account in winter is the likely enlargement of the initial ice avalanche volume by entrainment of snow along the trajectory.

Debris flow and lake outbursts

Results of the ANN classification were compared to ground truth data obtained by visual interpretation of the Landsat-TM scene combined with a debris layer automatically derived from topographic maps by the Swiss Federal Office of Topography (Swisstopo 2003). However, availability or generation of reliable and congruent ground truth is a major obstacle for measuring the classification accuracy (e.g. subjective interpretation of debris cover for production of topographic maps, or temporal changes caused by a 5-year time lag between ground truth acquisition and remote sensing data used). The accuracy of the ANN classification alone was not acceptable. The integration of slope ranges could improve the classification but still did not lead to satisfactory results.

For the detection of steep debris reservoirs based on very-high resolution remote sensing data, a test area near lake Gelmen was chosen. Fig. 6 shows the results of the detection method based on IKONOS imagery. Visual analysis of the image suggests that the classification algorithm provides accurate results. An exact quantification of the classification accuracy is difficult due to missing reference data but it may be estimated to 80 to 90%. Notably, only small parts of the large debris accumulations fall into the critical range of 27° or steeper, usually the uppermost parts of talus slopes. As can be inferred from Figs. 7 and 8, there is a scale difference between DEM and satellite data with spatial resolutions of 25 m and 1 m, respectively. Intersection of classification and DEM-derived slope values thus introduces, to a certain degree, a mixed-pixel problem but related negative effects are limited here according to a series of random tests performed.

For modeling a debris flow, a contact zone between a rock wall and a steep talus slope was selected from the classification (Fig. 7). Such zones have repeatedly been found to be typical for debris flow initiation (Rickenmann & Zimmermann 1993, Wilkerson & Schmid 2003). The trigger location is at the top of a large talus slope, and the erosion potential of a debris flow is thus considerable. In comparable talus slopes,

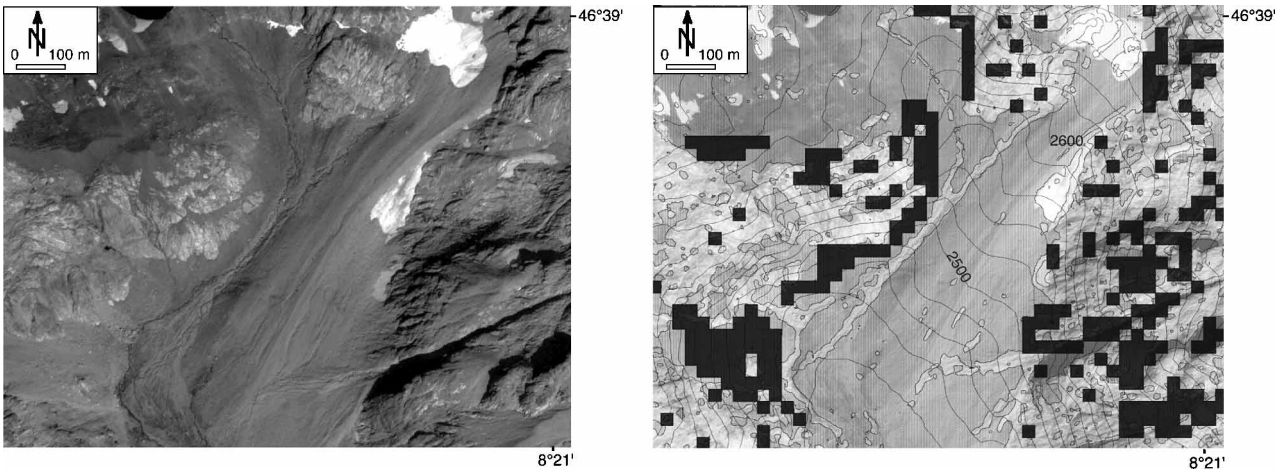

Fig. 6. IKONOS panchromatic image from 17 September 2000, with 1-m spatial resolution of a periglacial area with mixed presence of large talus slope, debris and bedrock (left). Potential debris flow initiation zones (black) are based on the classification of debris reservoirs (grey) and bedrock/sporadic debris (light grey).

bedrock depth can be several tens of meters, and in large neoglacial moraines up to more than 100 m (Haeberli et al. 2001, Huggel et al. 2003b). However, the availability of water or the flow dynamics are the limiting factors for the debris flow size rather than the sediment supply of the talus slope. Snow patches present at contact zones between rock wall and talus slope (Fig. 7) can be a source of water for debris flow initiation (Haeberli et al. 1991). Channel debris yield rates in deep taluses have been reported as 15 to 30 m^3/m (Hungr et al. 1984) whereas yield rates of several hundred m^3/m are generally observed only in connection with lake outbursts when water is not a limiting factor (Haeberli et al. 1989, O'Connor et al. 2001, Huggel et al. 2002). According to the above estimates and based on a talus slope length of 2250 m, the maximum debris flow size would be in the range of 34,000 to 68,000 m^3. Based on the modeled runout distance, the simulated debris flow reaches lake Gelmen. There are no other structures potentially affected before the flow reaches lake Gelmen (Fig. 7).

A second debris flow of slightly different conditions was modeled in the same Gelmen catchment further to the west (Fig. 8). The debris flow is triggered at the top of a similar but smaller talus slope. The model suggests that the debris flow reaches the periglacial lake immediately below, which has formed in the cirque after glacier recession. Though such a debris flow is probably of limited size (channel length of 200 m, estimated maximum flow size of *c*.3000 to 6000 m^3) and energy dissipation is not directed straight to the dam outflow, an adverse impact on the lake cannot be excluded. The slope of the inflowing mass is rather steep (25°). The lake has a considerable area of 28,000 m^2, with a probable volume of 150,000 to 300,000 m^3 of water. Based on analysis of the IKONOS image, the lake is dammed by morainic sediment, with bedrock depth probably being not more than a few meters. Bedrock is exposed at the surface *c*.40 m downstream from the dam crest. An overflow channel has developed. A potential impact wave by an inflowing debris flow and subsequent overspill of the dam could cause erosion of the sediment at the dam. The slope downstream of the overflow is 15° to 20°, with a smaller drop of 30°, and then it enters the flow channel of the debris flow described above. The size of a possible debris flow from a lake outburst depends mainly on whether the lake dam is fully breached. According to analysis of the IKONOS image, it is more likely that the breaching process is stopped when the bedrock is reached. Nevertheless, an outburst volume of *c*.50,000 m^3 could be sufficient to trigger a debris flow of *c*.100,000 to 150,000 m^3. Such a debris flow would probably reach lake Gelmen and enter it at a slope of 10°.

Process interactions

The Gauli-Grueben region was selected to demonstrate the importance of modeling potential process interactions. The geographic name Grueben is used for the glacier as well as for the lake at the bottom of the glacier. Historically, two main lake outbursts were recorded from lake Grueben. Both events, in 1921 and 1941, were related to ice masses damming the lake, which eventually provoked the outbursts. The 1941 event caused damage along the flow channel and particularly in Handegg, where the Grimsel Pass road was destroyed. Since then, the Grueben glacier has predominantly been in retreat and no further catastrophic events have been recorded. Between 1950 and 1954, the hydropower company KWO constructed a water intake at both lake Grueben and Grueben glacier. These water intakes are presently still providing water for the larger Grimsel hydropower system.

Today, the glacier is located less than 100 m from lake Grueben. The modeling performed suggests several potential ice avalanches from the Grueben cirque reaching the lake. Two main avalanche trajectories can be roughly distinguished, one entering lake Grueben from the north and a second one from the south. Both inflow directions are approximately perpendicular to the longitudinal axis of the lake, which results in a stronger dissipation of (wave) energy at the opposite bank than at the lake outflow. Inflow slopes are *c*.10° for the northern and *c*.20° for the southern avalanche. The effect of an impact at the lake outflow is not clear. However, in consideration of the lake size (60,000 m^2),

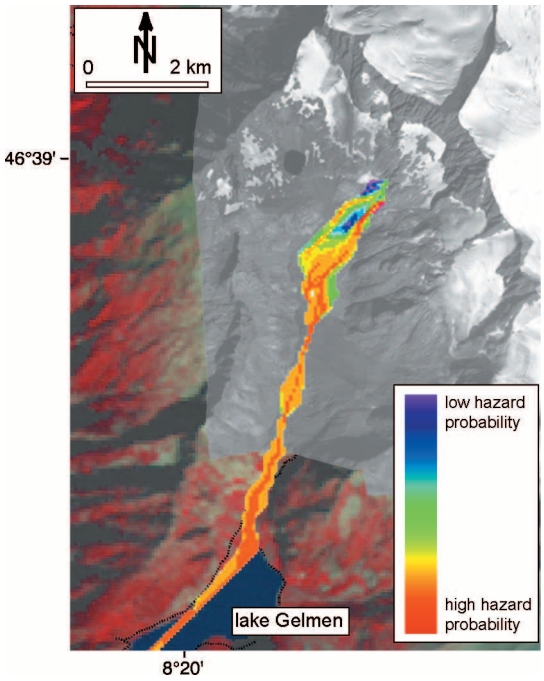

Fig. 7. Model of a potential debris flow initiated at the contact zone of a large debris reservoir with bedrock. The color range of the flow model relates to the probability of a certain cell to be affected. The model is projected on the IKONOS panchromatic image from 17 September 2000, and at the edge on the Landsat-TM image taken 31 August 1998.

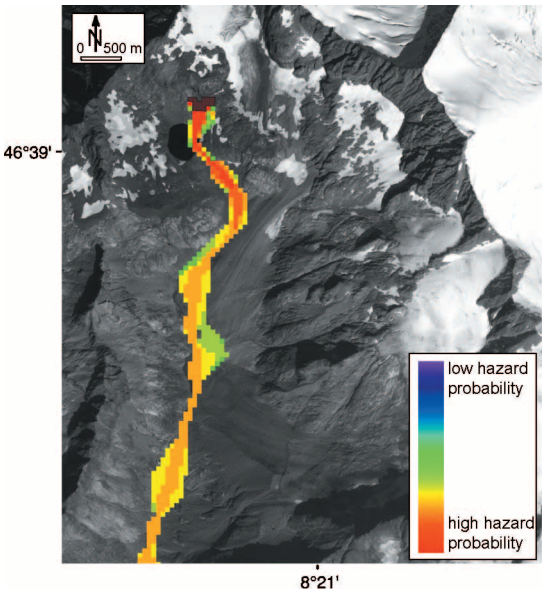

Fig. 8. Modeled initial debris flow and subsequent lake outburst. Debris flow starting cells are shown in brown, the color range of the flow model relates to the probability of a certain cell to be affected. The model is projected on the IKONOS panchromatic image from 17 September 2000.

the ratio, H, would likely be between 1:10 and 1:100 in the case of an impact by a major ice avalanche. Lake overtopping is then a realistic scenario. Recent cases have thereby shown that small overflows can also be sufficient to trigger debris flows with severe effects (Huggel et al. 2003b). The lake is constrained by bedrock such that we assume stable dam conditions. Downstream of the lake, there is a 700-m long section of unconsolidated sediment which could possibly be mobilized by such an event. The modeled debris flow reaches Handegg and the Grimsel Pass highway (Fig. 9).

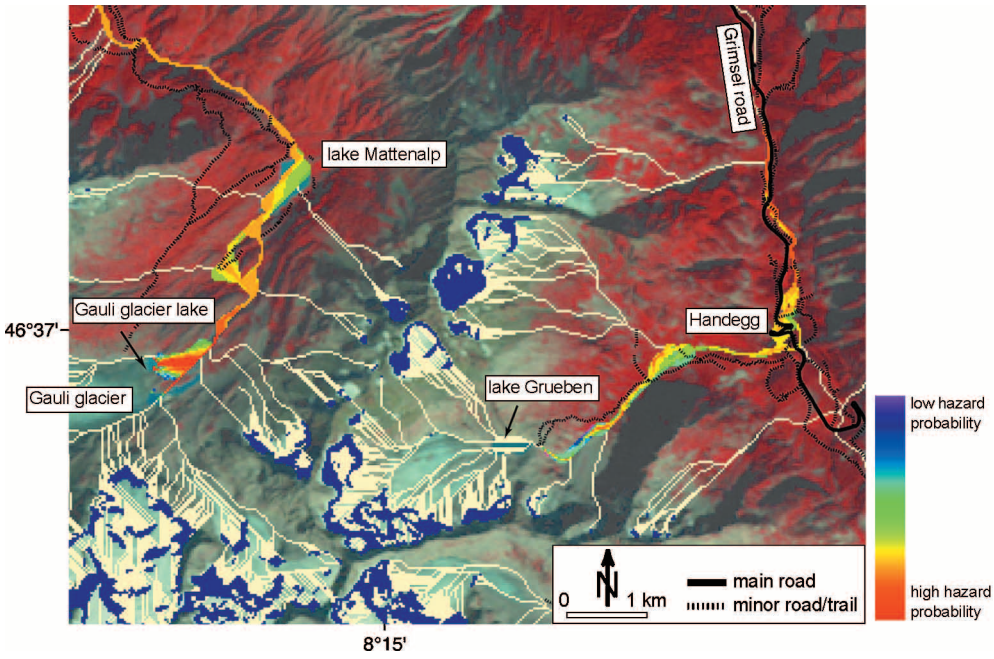

Fig. 9. Modeled process interactions within the study region showing potentially unstable glacier areas (blue), ice avalanches (white) and debris flows resulting from lake failure (color range). The color range of the flow model relates to the probability of a certain cell to be affected. Potentially endangered traffic routes, roads, or hiking areas can be observed. The models are projected on the Landsat-TM image from 31 August 1998.

A second focus of process interaction modeling is directed on the Gauli glacier area. The Gauli glacier, currently with an area of 13.7 km^2, has substantially retreated in recent years. In the glacier forefield, mainly consisting of bedrock, two main lakes have formed (and recently joined) and are presently increasing roughly proportional to the glacier recession rate (Fig. 10). Further downstream, a reservoir lake called Mattenalp is dammed by a 25-m high weight dam. A water intake serves the Grimsel hydropower system. The model indicated several possible process interactions. Two ice avalanches were modeled into the southern part of Gauli glacier lake from the south and south-west, with slopes entering the lake at 30° and 15° to 20°, respectively. Due to the inflowing direction and slope, it is assumed that the south-western ice avalanche has a higher potential for producing an impact wave and subsequent outburst flood. Predominant bedrock conditions and moderate slopes between the Gauli glacial lake and lake Mattenalp make a significant flow increase by sediment entrainment rather unlikely. According to the model, lake Mattenalp can be hit either by such a flood or an ice avalanche from a small glacier at Steinlauihorn, 2 km south-east of lake Mattenalp. In the absence of a detailed engineering study, we consider the possibility of severe damage of the weight dam at lake Mattenalp by such inflowing mass movements unlikely. However, depending on the dam freeboard, an overtopping wave cannot be excluded. The size of the subsequent debris flow (or flood) largely depends on the overtopping water volume and is not further analyzed here. The debris flow was routed downstream by the model. The runout distance is related to the sediment concentration in the flow, and therefore also depends on the available sediment in the flow trajectory.

Discussion

This paper presents a concept on the modeling potential of the interaction of hazardous processes in glacial and periglacial environments based on remote sensing data and GIS. The emphasis is thus on developing and demonstrating techniques and tools for first-order hazard assessments, rather than on the analysis of the actual hazards encountered in the selected region. Regional-scale studies such as the present one enable us to indicate where complex hazard interactions can possibly be found. In doing so, they prepare the field for more detailed analyses which are needed for a thorough study of processes and associated parameters and effects. Consequently, this relates as follows to the processes treated here.

Fig. 10. Gauli glacier tongue with the proglacial lake. The width of the valley bottom covered by the lake is *c.*700 m. Arrows indicate the flow trajectories of ice avalanches as modeled and shown in Fig. 9 (photo: H. Glauser, July 2003).

Ice avalanches

Remote sensing imagery with spatial resolution in the range of 20 to 30 m and appropriate near-infrared spectral resolution allows mapping of glacier ice, and could indicate recent major break-off zones or ice avalanche deposits. IKONOS imagery, representing the new generation of very-high resolution space-borne data, allows for studying crevasse systems and more details on break-off zones. Discrimination of further characteristics, such as surrounding bed conditions, meltwater presence or general ice structure, and ice volume estimates, may thus be facilitated. However, investigation of glacier stability and break-off conditions (avalanche starting conditions) is extremely difficult and fairly uncertain, particularly for steep or hanging glaciers. In general, it remains highly complex to predict the avalanche starting volume or the time of failure. In selected critical cases, direct measurements (e.g. ice deformation rates) can be a viable method of prediction (Wegmann et al. 2003). In most other cases and on a regional scale, assessments have to be based largely on empirical experience and topographic information (Alean 1985). Ice avalanche modeling is based here on topography-related hydrological flow routing. Salzmann et al. (2004) have shown that this GIS-based approach yields hazard delineations comparable to Voellmy-Salm based models (Margreth & Funk 1999). In general, modeling of flow dynamics of ice avalanches remains a poorly developed area.

Lake outbursts

The investigation of lake-outburst hazards applies a strategy of lake detection followed by assessment of outburst trigger factors, dam stability and breach mechanism, and downstream flow processes. Indicators can be used for evaluation of lake and dam stability (Huggel et al. 2002, J.M. Reynolds et al., unpublished data). Dam breach and peak discharge are not explicitly analyzed here but we suggest consideration of earlier contributions based on empirical information (Huggel et al. 2002). More sophisticated models, including physically based formulations and related publicly available software for derivation of flow hydrographs, have been presented by Walder & O'Connor (1997) and Fread (1991), respectively. Assessment of downstream flow hazards is achieved here by a model which provides potentially endangered areas in terms of probability. However, the model does not directly

give any information on the expected debris flow volume, amount of sediment eroded and deposited, or on flow depth and velocity (Huggel et al. 2003b). These parameters can be estimated by empirical models, or alternatively or complementarily by physically-based models. A main obstacle with the application of physically-based models in this area is the difficulty of assessing parameters required for models, e.g. the volume of water released from the lake. Assumptions which need to be made can have a large degree of uncertainty. In particular, in glacial and periglacial areas, collection of field data may be impossible or prohibitive in terms of finance, time or personal risk. For the determination of the runout distance of the outburst-related debris flow, relying on a 1-parameter model is a simplification but one that is viable for regional-scaled first order assessments (Huggel et al. 2003a). Models based on energy dissipation or volume conservation approaches can be applied for more detailed studies (Hirano et al. 1997, Zimmermann et al. 1997).

Periglacial debris flows

The method presented to detect steep debris reservoirs based on IKONOS imagery allows remote assessment of potential debris flow initiation areas. Results show a high accuracy compared to the less successful combined ANN/slope classification. The ANN classification indicated that spatial resolution of remote sensing data is an essential element. In fact, due to the spectral similarity between debris and bedrock, the latter had to be distinguished by a measure of texture at a spatial resolution higher than Landsat-TM allows for. The scale difference between 1-m spaced IKONOS imagery and 25-m spaced DEM data can theoretically induce classification errors. According to the algorithm used, a 25-m spaced slope cell (between 27° and 38°) is classified as 'debris with critical slope value' if there is a majority of 1-m spaced debris cells intersected with this cell. Based on this, the scale difference theoretically induces an error $< 50\%$. Larger, connected areas of debris have smaller errors than areas with small debris patches. Analyses have shown that such errors do not significantly affect the subsequent debris flow modeling. An interesting question, not investigated here, is the minimal spatial resolution necessary for successful detection of debris reservoirs. If, for instance, images with a 2.5 or 5 m resolution (e.g. corresponding to satellite sensors SPOT-5 Pan or IRS-Pan, respectively) yield acceptable results, a more economic and efficient solution could be achieved due to the larger area covered by a satellite scene and the lower price per km^2 (*c*.US$1 to 1.5 per km^2 for SPOT-5/IRS compared to US$20–30 per km^2 for IKONOS). As an alternative to IKONOS, though on comparable expense, QuickBird panchromatic imagery of 0.6 m spatial resolution could be used. If an area under investigation is covered by recent aerial photography this may be the most economic and practical solution. However, in areas without any aerial photography, IKONOS and QuickBird data may still be a more economic or even the only solution, particularly if political, military/strategic, or technical restrictions are involved.

Process interactions

To date, the problem of process interactions has seldom been addressed with respect to glacial hazards. This study intends to achieve systematic modeling of such interactions. As for the modeling of individual processes, a regional-scale range was chosen. In consideration of the complexity of interacting processes, the model requires an expert to interfere and analyze the conditions at the interface of interacting processes. The most imminent and widespread hazards emerge from mass movements into glacial lakes. Here, ice avalanches and debris flows were considered as inflow processes, whereas snow avalanches, rockfall or landslides were beyond the scope of the study. The model is capable of indicating where critical situations may be found. Based on reasonable assumptions, findings from recent studies and digital terrain data, a first-order assessment of the effects on the lake was conducted. For a critical case, the flow dynamics of the incoming mass movement and the effects on wave length and height in the lake have to be investigated. Though considerable progress has been made with respect to wave-generating processes (Fritz 2002, Walder et al. 2003), the problem generally remains highly complex. The inflowing mass volume is one of the most critical parameters that needs to be assessed. However, prediction of the potential failing mass volume is fraught with uncertainty, particularly for ice avalanches. It is therefore suggested here that different scenarios of mass failure and flow are defined including a worst-case, which typically assumes instability of the whole hanging glacier in the case of ice avalanches. Other process interactions, such as river damming by ice avalanches or debris flows, should also be taken into account. Such ice avalanche dams often burst by sudden failure unless the dam is very large (several hundred meters long), highly compacted, and with a significant content of debris (Kääb et al. 2003a). Empirical relations for peak discharge estimates of sudden ice dam failures have been provided by, for example, Haeberli (1983) and Walder & Costa (1996). In view of the integrative hazard assessment aimed at here, information on infrastructure was included. Individual buildings were not considered since that would require a more detailed assessment than performed here.

Perspectives

The use of recent satellite imagery together with simple but robust models is an effective tool to address rapid changes in glacial and periglacial environments and to assess the related hazards. Climate change can significantly affect the conditions in glacial and periglacial areas, though the related effects and processes are often not well understood. Degradation of permafrost (Haeberli et al. 1997) or ice-cored moraines (Richardson & Reynolds 2000b) can increase the related hazards. As far as hanging glaciers are concerned, knowledge on their reaction to rising temperatures is limited. The small number of studies available indicates a potential reduction in stability due to changes in the thermal and hydrological regime of the glacier (Lüthi & Funk 1997, Haeberli et al. 1999). In periods of glacier recession, glacial

lake formation tends to increase (Richardson & Reynolds 2000a, Kääb et al., in press). In the region of the present study, two striking examples of lake formation and rapid growth which modify and intensify the hazard situation are found (i.e. Gauli and Trift glacial lakes) (Fig. 1), and stress the importance of periodic observations (<1 year in these cases). glacier retreat also continues to expose debris accumulations. Hazardous future developments may be anticipated by assessing glaciers with sediment beds (Maisch et al. 1999, Zemp 2002) and estimating related slopes.

Though the methodological strategy presented here is designed to meet the change in glacial and periglacial areas, techniques may be subject to adjustment to new data available in the future. Recent very-high resolution satellite sensors such as IKONOS, QuickBird or SPOT-5 have already widened the horizon of application techniques (Goward et al. 2003, Huggel et al. 2003c). The development of new sensors with high spatial and spectral resolution is continuing, and DEM quality and spatial resolution are expected to be improved (Kääb et al. 2003b). On the other hand, the production of increasingly large data volumes may make adequate techniques for data handling and retrieval of information over large areas an increasingly more critical issue.

Finally, a note on user perspectives: commercially oriented practice still strongly relies on aerial photography. The methods presented here are basically compatible with aerial photography but the automatic procedures would then be lost. An exception is the method to detect steep debris reservoirs, since IKONOS panchromatic imagery is comparable to aerial photography. In addition to this, the models presented here are relatively simple in their use and thus favor the application in practice. Hence, the models may be a tool for practitioner institutions to assess potential hazard process interactions in glacial and periglacial environments as well as their likely effects on downstream areas.

Acknowledgements.—This study was made possible thanks to the Swiss National Science Foundation, as part of the NF21-59045.99 project. We greatly acknowledge the support by Frank Paul and Sonja Oswald, careful comments by Wilfried Haeberli and stimulating discussions with Andreas Zweifel. We are furthermore grateful for information provided by KWO (M. Ursin). Finally, we are indebted to two anonymous reviewers and the Editor Bernd Etzelmüller for their helpful comments.

Manuscript submitted 9 February 2004; accepted 1 April 2004

References

Alean, J. 1985. Ice avalanches: some empirical information about their formation and reach. *Journal of Glaciology* 31, 324–333.

Bachmann, A. 2001. *GIS-based wildland fire risk analysis*. PhD thesis, Department of Geography. University of Zurich, Zurich.

Bathurst, J.C., Crosta, G.B., García-Ruiz, J.M., Guzzetti, F., Lenzi, M.A. & Ríos Aragüés, S. 2003. DAMOCLES: debris-fall assessment in mountain catchments for local end-users. Rickenmann, D. & Chen, C.L. (eds.) *Debris-Flow Hazards Mitigation: Mechanics, Prediction and Asssessment*, 1073–1083. Third International DFHM Conference, Davos, Switzerland, 10–12 September 2003. Millpress, Rotterdam.

Bishop, M.P., Shroder, J.F., Jr & Hickman, B.L. 1999. SPOT Panchromatic imagery and neural networks for information extraction in a complex mountain environment. *Geocarto International* 14, 19–28.

Clague, J.J. & Evans, S.G. 2000. A review of catastrophic drainage of moraine-dammed lakes in British Columbia. *Quarternary Science Reviews* 19, 1763–1783.

Dial, G., Bowen, H., Gerlach, F., Grodecki, J. & Oleszczuk, R. 2003. IKONOS satellite, imagery, and products. *Remote Sensing of Environment* 88, 23–36.

Deline., P., Chiarle, M. & Mortara, G. 2002. The frontal ice avalanche of Frebouge Glacier (Mont Blanc Massif, Valley of Aosta, NW Italy) on 18 September 2002. *Geografia Fisica e Dinamica Quarternaria* 25, 101–104.

Dutto, F., Godone, F. & Mortara, G. 1991. L'écroulement du Glacier superieur de Coolidge. *Revue Géographique Alpine* 79, 7–18.

Evans, S.G. & Clague, J.J. 1994. Recent climatic change and catastrophic geomorphic processes in mountain environments. *Geomorphology* 10, 107–128.

Fread, D.L. 1991. *Breach: an erosion model for earthen dam failures*. National Weather Service, NOAA, Silver Spring, MD.

Fritz, H.M. 2002. *Initial phase of landslide generated impulse waves*. Mitteilungen der VAW/ETHZ, 178, Zürich.

Funk, M. & Minor, H.E. 2001. Eislawinen in den Alpen: Erfahrungen mit Schutzmassnahmen und Früherkennungmethoden. *Wasserwirtschaft* 91, 362–368.

Goward, S.N., Townshend, J.R.G., Zanoni, V., Policelli, F., Stanley, T., Ryan, R., Holekamp, K., Underwood, L., Pagnutti, M. & Fletcher, R. 2003. Acquisition of earth science remote sensing observations from commercial sources: lessons learned from the Space Imaging IKONOS example. *Remote Sensing of Environment* 88, 209–219.

Greminger, P. 2003. Managing the risks of natural hazards. Rickenmann, D. & Chen, C.L. (eds.) *Debris-Flow Hazards Mitigation: Mechanics, Prediction and Asssessment*, 39–56. Third International DFHM Conference, Davos, Switzerland, 10–12 September 2003. Millpress, Rotterdam.

Haeberli, W. 1983. Frequency and characteristics of glacier floods in the Swiss Alps. *Annals of Glaciology* 4, 85–90.

Haeberli, W. 1996. On the morphodynamics of ice/debris-transport systems in cold mountain areas. *Norsk Geografisk Tidsskrift* 50, 3–9.

Haeberli, W. & Burn, C.R. 2002. Natural hazards in forests: glacier and permafrost effects as related to climate change. Sidle, R.C. (ed.) *Environmental Change and Geomorphic Hazards in Forests*, 167–202. IUFRO Research Series 9. CABI Publishing, Wallingford/New York.

Haeberli, W., Alean, J.-C., Müller, P. & Funk, M. 1989. Assessing the risks from glacier hazards in high mountain regions: some experiences in the Swiss Alps. *Annals of Glaciology* 13, 77–101.

Haeberli, W., Rickenmann, D. & Zimmermann, M. 1991. *Murgänge. In Ursachenanalyse der Hochwasser 1987, Ergebnisse der Untersuchungen*. Mitteilung des Bundesamtes für Wasserwitschaft, 4, Bern.

Haeberli, W., Wegmann, M. & Vonder Mühll, D. 1997. Slope stability problems related to glacier shrinkage and permafrost degradation in the Alps. *Eclogae Geologicae Helvetiae* 90, 407–414.

Haeberli, W., Kääb, A., Hoelzle, M., Bösch, H., Funk, M., Vonder Mühll, D. & Keller, F. 1999. *Eisschwund und Naturkatastrophen im Hochgebirge*. Schlussbericht NFP31. vdf Hochschulverlag an der ETH, Zürich.

Haeberli, W., Kääb, A., Vonder Mühll, D. & Teysseire, P. 2001. Prevention of outburst floods from periglacial lakes at Gruben Glacier, Valais, Swiss Alps. *Journal of Glaciology* 47, 111–122.

Haefeli, R. 1966. Note sur la classification, le mécanisme et le contrôle des avalanches de glaces et des crues glaciaires extraordinaires. *IAHS Publication* 69, 316–325.

Hall, D.K., Chang, A.T.C. & Siddalingaiah, H. 1988. Reflectances of glaciers as calculated using Landsat 5 Thematic Mapper data. *Remote Sensing of Environment* 25, 311–321.

Heinimann, H.R., Hollenstein, K., Kienholz, H., Krummenacher, B. & Mani, P. 1998. *Methoden zur Analyse und Bewertung von Naturgefahren*. Bundesamt für Umwelt, Wald und Landschaft (BUWAL), Bern.

Hirano, M., Harada, T., Banihabib, M.E. & Kawahara, K. 1997. Estimation of hazard area due to debris flow. Chen, C.-L. (ed.) *Debris-Flow Hazard Mitigation: Mechanics, Prediction, and Assessment*, 697–706. Proceedings of the First International Conference, San Francisco, California, 7–9 August 1997. American Society of Civil Engineers, Reston.

Huber, A. 1980. *Schwallwellen in Seen als Folge von Felsstürzen*. Mitteilungen der VAW/ETHZ 47, Zürich.

Huggel, C., Kääb, A., Haeberli, W., Teysseire, P. & Paul, F. 2002. Remote sensing based assessment of hazards from glacier lake outbursts: a case study in the Swiss Alps. *Canadian Geotechnical Journal* 39, 316–330.

Huggel, C., Kääb, A., Haeberli, W. & Krummenacher, B. 2003a. Regional-scale GIS-models for assessment of hazards from glacier lake outbursts:

evaluation and application in the Swiss Alps. *Natural Hazards and Earth System Sciences* 3, 647–662.

Huggel, C., Kääb, A. & Haeberli, W. 2003b. Regional-scale models of debris flows triggered by lake outbursts: the 25 June 2001 debris flow at Täsch (Switzerland) as a test study. Rickenmann, D. & Chen, C.-L. (eds.) *Debris-Flow Hazards Mitigation: Mechanics, Prediction and Asssessment*, 1051–1062. Third International DFHM Conference, Davos, Switzerland, 10–12 September 2003. Millpress, Rotterdam.

Huggel, C., Oswald, S., Kääb, A., Haeberli, W., Polkvoj, A. & Galushkin, I. 2003c. Application potential of very-high resolution remote sensing data (QuickBird) for high-mountain hazards: a case study with the 2002 rock/ice avalanche disaster in the Russian Caucasus. Geomorphic Hazards. International Association of Geomorphologists *Towards the Prevention of Disasters*, 106–107. IAG Regional Geomorphology Conference, Mexico City, 27 October–2 November 2003, Abstracts. Talleres de Editorial Cromocolor, S.A. De C.V., Mexico.

Hungr, O., Morgan, G.C. & Kellerhals, P. 1984. Quantitative analysis of debris hazards for design of remedial measures. *Canadian Geotechnical Journal* 21, 663–677.

Jacobs, J.D., Simms, E.L. & Simms, A. 1997. Recession of the southern part of Barnes Ice Cap, Baffin Island, Canada, between 1961 and 1993, determined from digital mapping of Landsat TM. *Journal of Glaciology* 43, 98–102.

Jenson, S.K. & Domingue, J.O. 1988. Extracting topographic structure from digital elevation data for geographic information system analysis. *Photogrammetric Engineering and Remote Sensing* 54, 1593–1600.

Kääb, A., Wessels, R., Haeberli, W., Huggel, C., Kargel, J.S. & Khalsa, S.J.S. 2003a. Rapid ASTER imaging facilitates timely assessment of glacier hazards and disasters. *EOS Transactions, AGU* 84, 117, 121.

Kääb, A., Huggel, C., Paul, F., Wessels, R., Raup, B., Keiffer, H. & Kargel, J. 2003b. Glacier monitoring from ASTER imagery: accuracy and applications. Wunderle, S. (ed.) *EARSeL eProceedings 2, 1/2003, Observing our Cryosphere from Space*, 43–53. EARSeL, BIS-Verlag, Oldenburg.

Kääb, A., Reynolds, J.M. & Haeberli, W. Glacier and permafrost hazards in high mountains. Huber, U.M., Reasoner, M.A. & Bugmann, B. (eds.) *Global Change and Mountain Regions: a State of Knowledge Overview*. Advances in Global Change Research. Kluwer Academic Publishers, Dordrecht. In press.

Körner, H.J. 1983. Zur Mechanik der Bersturzströme vom Huascaran, Peru. *Hochgebirgsforschung* (Innsbruck) 6, 71–110.

Lliboutry, L., Morales Arnao, B. & Schneider, B. 1977. Glaciological problems set by the control of dangerous lakes in Cordillera Blanca, Peru. I. Historical failures of morainic dams, their causes and prevention. *Journal of Glaciology* 18, 239–254.

Lüthi, M. & Funk, M. 1997. Wie stabil ist der Hängegletscher am Eiger? *Spektrum der Wissenschaft* May, 21–24.

Maisch, M., Haeberli, W., Hoelzle, M. & Wenzel, J. 1999. Occurrence of rocky and sedimentary glacier beds in the Swiss Alps as estimated from glacier-inventory data. *Annals of Glaciology* 28, 231–235.

Margreth, S. & Funk, M. 1999. Hazard mapping for ice and combined snow/ice avalanches – two case studies from the Swiss & Italian Alps. *Cold Regions Science and Technology* 30, 159–173.

Marks, D., Dozier, J. & Frew, J. 1984. Automated basin delineation from digital elevation data. *Geo Processing* 2, 299–311.

Müller, D. 1995. *Auflaufen und Überschwappen von Impulswellen an Talsperren*. VAW/ETHZ 137, Zürich.

Oberholzer, P., Vonder Mühll, D. & Ansorge, J. 2003. Shallow structure of the Rossboden Glacier and its moraine dam (Valais, Swiss Alps). *Eclogae Geologicae Helvetiae* 96, 299–312.

O'Callaghan, J.F. & Mark, D.M. 1984. The extraction of drainage networks from digital elevation data. *Computer Vision Graphics and Image Proceedings* 28, 323–344.

O'Connor, J.E., Hardison, III, J.H. & Costa, J.E. 2001. *Debris Flows from Failures of Neoglacial-Age Moraine Dams in the Three Sisters and Mount Jefferson Wilderness Areas, Oregon*. US Geological Survey Professional Paper 1606. USGS, Reston (VA).

Oswald, S. 2001. *Kartierung und Modellierung von periglazialen Murgängen*. Diploma thesis, Department of Earth Sciences. ETH, Zürich.

Pao, Y.H. 1989. *Adaptive Pattern Recognition and Neural Networks*. Addison-Wesley Publishing Company, Massachusetts.

Paul, F., Kääb, A., Maisch, M., Kellenberger, T. & Haeberli, W. 2002. The new remote sensing derived Swiss glacier inventory. I. Methods. *Annals of Glaciology* 34, 355–361.

Paul, F., Huggel, C. & Kääb, A. 2004. Combining multispectral satellite data and a digital elevation model for mapping of debris-covered glaciers. *Remote Sensing of Environment* 89, 510–518.

Petrascheck, A. & Kienholz, H. 2003. Hazard assessment and mapping of mountain risks in Switzerland. Rickenmann, D. & Chen, C.-L. (eds.) *Debris-Flow Hazards Mitigation: Mechanics, Prediction and Assessment*, 25–38. Third International DFHM Conference, Davos, Switzerland, 10–12 September 2003. Millpress, Rotterdam.

Pierson, T.C. & Scott, K.M. 1985. Downstream dilution of a lahar: transition from debris flow to hyperconcentrated streamflow. *Water Resources Research* 21, 1511–1524.

Reynolds, J.M. 1992. The identification and mitigation of glacier-related hazards: examples from the Cordillera Blanca, Peru. McCall G.J.H., Laming D.J.C. & Scott S.C. (eds.) *Geohazards Natural and Man-Made*, 143–157. Chapman and Hall, London.

Richardson, S.D. & Reynolds, J.M. 2000a. An overview of glacial hazards in the Himalayas. *Quaternary International* 65/66, 31–47.

Richardson, S.D. & Reynolds, J.M. 2000b. Degradation of ice-cored moraine dams: implications for hazard development. *IAHS Publication* 264, 187–97.

Rickenmann, D. & Zimmermann, M. 1993. The 1987 debris flows in Switzerland: documentation and analysis. *Geomorphology* 8, 175–189.

Röthlisberger, H. 1981. Eislawinen und Ausbrüche von Gletscherseen. *Jahrbuch der Schweizerischen Naturforschen Gesellschaft*, wissenschaftlicher Teil 1978, 170–212.

Salzmann, N., Kääb, A., Huggel, C., Allgöwer, B. & Haeberli, W. 2004. Assessment of the hazard potential of ice avalanches using remote sensing and GIS-modeling. *Norsk Geografisk Tidsskrift–Norwegian Journal of Geography* 58:2, 74–84.

Swisstopo 2003. Online: http://www.swisstopo.ch. 18 September 2003. 99 pp.

Takahashi, T. 1981. Estimation of potential debris flows and their hazardous zones; soft countermeasures for a disaster. *Journal of Natural Disaster Science* 3, 57–89.

Tarboton, D.G., Bras, R.L. & Rodriguez-Iturbe, I. 1991. On the extraction of channel networks from digital elevation data. *Hydrological Processes* 5, 81–100.

Vischer, D.L. & Hager, W.H. 1998. *Dam Hydraulics*. John Wiley and Sons, Chichester.

Walder, J.S. & Costa, J.E. 1996. Outburst floods from glacier-dammed lakes: the effect of mode of lake drainage on flood magnitude. *Earth Surface Processes and Landforms* 21, 701–723.

Walder, J.S. & O'Connor, J.E. 1997. Methods for predicting peak discharge of floods caused by failure of natural and constructed earthen dams. *Water Resources and Research* 33, 2337–2348.

Walder, J.S., Watts, P., Sorensen, O.E. & Janssen, K. 2003. Water waves generated by subaerial mass flows. *Journal of Geophysical Research* 108:(B5), 2236–2255.

Watts, P. & Walder, J.S. 2003. Evaluating tsunami hazards from debris flows. Rickenmann, D. & Chen, C.L. (eds.) *Debris-Flow Hazards Mitigation: Mechanics, Prediction and Asssessment*, 1245–1256. Third International DFHM Conference, Davos, Switzerland, 10–12 September 2003. Millpress, Rotterdam.

Wegmann, M., Funk, M., Flotron, A. & Keusen, H. 2003. Movement studies to forecast the time of breaking off of ice and rock masses. Zschau, J. & Küppers, A. (eds.) *Early Warning Systems for Natural Disasters Reduction*, 565–568. Springer, Potsdam.

Wilkerson, F.D. & Schmid, G.L. 2003. Debris flows in Glacier National Park, Montana: geomorphology and hazards. *Geomorphology* 55, 317–328.

Zemp, M. 2002. *GIS-basierte Modellierung der glazialen Sedimentbilanz*. Diploma thesis, Department of Geography. University of Zurich, Zurich.

Zimmermann, M. & Haeberli, W. 1992. Climatic change and debris flow activity in high mountain areas: a case study in the Swiss Alps. *Catena Supplement* 22, 59–72.

Zimmermann, M., Mani, P., Gamma, P., Gsteiger, P., Hunziker, G. & Heiniger, O. 1997. *Beurteilung der Murganggefährdung mit Hilfe eines Geographischen Informationssystems. Analyse der räumlichen Entwicklung infolge von Klimaänderungen*. Schlussbericht NFP31 (Projekt 4031–33253).